Delayed onset of brain edema and mislocalization of aquaporin-4 in dystrophin-null transgenic mice

Zsolt Vajda*†, Michael Pedersen‡, Ernst-Martin Füchtbauer§, Karin Wertz¶, Hans Stødkilde-Jørgensen‡, Endre Sulyok‖, Tamás Dóczi†, John D. Neely**, Peter Agre**, Jørgen Frøkiær*, and Søren Nielsen*††

*Water and Salt Research Center, University of Aarhus, DK-8000 Aarhus, Denmark; ‡MR Research Centre, Aarhus University Hospital, DK-8200 Aarhus, Denmark; §Institute of Molecular and Structural Biology, University of Aarhus, DK-8000 Aarhus, Denmark; ¶Max Planck Institute of Immunobiology, D-79011 Freiburg, Germany; †Department of Neurosurgery, University of Pécs, H-7624, Pécs, Hungary; ‖County Children's Hospital, H-7624, Pécs, Hungary; and **Department of Biological Chemistry, The Johns Hopkins University School of Medicine, Baltimore, MD 21205

Cerebral water accumulation was studied during induction of brain edema in dystrophin-null transgenic mice (*mdx-βgeo*) and control mice. Immunofluorescence and immunoelectron microscopic analyses of dystrophin-null brains revealed a dramatic reduction of AQP4 (aquaporin-4) in astroglial end-feet surrounding capillaries (blood–brain barrier) and at the glia limitans (cerebrospinal fluid–brain interface). The AQP4 protein is mislocalized, because immunoblotting showed that the total AQP4 protein abundance was unaltered. Brain edema was induced by i.p. injection of distilled water and 8-deamino-arginine vasopressin. Changes in cerebral water compartments were assessed by diffusion-weighted MRI with determination of the apparent diffusion coefficient (ADC). In dystrophin-null mice and control mice, ADC gradually decreased by 5–6% from baseline levels during the first 35 min, indicating the initial phase of intracellular water accumulation is similar in the two groups. At this point, the control mice sustained an abrupt, rapid decline in ADC to 58% ± 2.2% of the baseline at 52.5 min, and all of the animals were dead by 56 min. After a consistent delay, the dystrophin-null mice sustained a similar decline in ADC to 55% ± 3.4% at 66.5 min, when all of the mice were dead. These results demonstrate that dystrophin is necessary for polarized distribution of AQP4 protein in brain where facilitated movements of water occur across the blood–brain barrier and cerebrospinal fluid–brain interface. Moreover, these results predict that interference with the subcellular localization of AQP4 may have therapeutic potential for delaying the onset of impending brain edema.

Brain edema is associated with many intracranial neuropathological states, such as head trauma, ischemic brain injury, neoplasms, and metabolic diseases including systemic hyponatremia. Although much investigation has addressed the underlying molecular mechanisms and pathophysiology of brain edema, little is known about the regulation of water transport across the blood–brain barrier, the cerebrospinal fluid (CSF)–brain interface, and between extracellular and intracellular compartments in brain parenchyma.

It is well recognized that the aquaporin family of water channel proteins is the major pathway by which water rapidly crosses cell membranes (1). Manley *et al.* recently reported that AQP4 (aquaporin-4; ref. 18) negatively influences the outcome from brain edema (2), and other recent studies also have suggested that AQP4 contributes to the development of brain edema (3, 4). These observations are consistent with the distribution of AQP4 in brain, because the protein is expressed abundantly in a highly polarized distribution in ependymal cells and astroglial membranes facing capillaries and forming the glia limitans (5).

Decreased expression of AQP4 protein without changes in the AQP4 mRNA levels was reported recently in brains of *Dmd^mdx* mice (C57BL10 ScSn mdx), a strain carrying a spontaneous mutation that prevents expression of the longest isoform of dystrophin (6). α-Syntrophin (α-syn) is a member of the dystrophin-associated protein complex (DAP). A study of mice homozygous for targeted disruption of *α-syn* gene showed that the

protein is essential for localization of AQP4 protein in astrocyte end-feet membrane domains adjacent to brain capillaries (7). In contrast to findings in the *Dmd^mdx* mice (6), immunoblots of brain and cerebellar samples from the *α-syn* knockout mice revealed that AQP4 protein expression was quantitatively unchanged (7).

Diffusion-weighted MRI (DWI) has been used to evaluate the development of edema in a variety of neurological disorders including stroke (8), head trauma (9), and metabolic disturbances like systemic hyponatremia (10). This method allows the *in vivo* monitoring of changes in the ratio of extracellular to intracellular volume (11–13) and the development of cellular swelling or shrinkage (13–15) by measuring the apparent diffusion coefficient (ADC) of the tissue water.

In this study, expression and tissue localization of the AQP4 water channel protein were measured in the brains of dystrophin-null *mdx-βgeo* transgenic mice. In this model of Duchenne muscular dystrophy (16), the transgenic allele ensures that none of the known dystrophin genes and splice variants are expressed. Changes of the extracellular and intracellular compartments were measured in these animals by using diffusion-weighted MRI during the development of brain edema induced by systemic hyponatremia.

Materials and Methods

Animal Model. Studies were performed on 12- to 13-month-old female mice, weighing 28–32 g. The generation and characterization of the dystrophin-null *mdx-βgeo* mutation has been described (16). A different mouse line (Gl78), with insertion of the identical gene trap vector sequence into a different chromosome, served as age-matched control animals with the same genetic background (129Sv^Pas) (16). Age-matched NMRI mice were used as a second, non-transgenic control. The animals were maintained on standard rodent diet with free access to water. All procedures were performed according to the guidelines of the Danish Medical Research Council.

Experimental Procedures. The mice were anesthetized with pentobarbital sodium (7.5 mg/kg i.p.) and positioned in a specially designed, plastic, stereotactic frame, which allowed the exact repositioning of the animal into the magnet to obtain data from the same coronal slices during the whole experimental procedure. Body temperature during the MRI experiments was maintained by using a warm water pad.

DWI. All imaging experiments were performed on a 7 T MRI system (Varian), as described (15). Diffusion-weighted images were acquired in three consecutive coronal slices, covering the

---

Abbreviations: AQP4, aquaporin-4; DWI, diffusion-weighted imaging; α-syn, α-syntrophin; ADC, apparent diffusion coefficient; DAP, dystrophin-associated protein complex; CSF, cerebrospinal fluid.

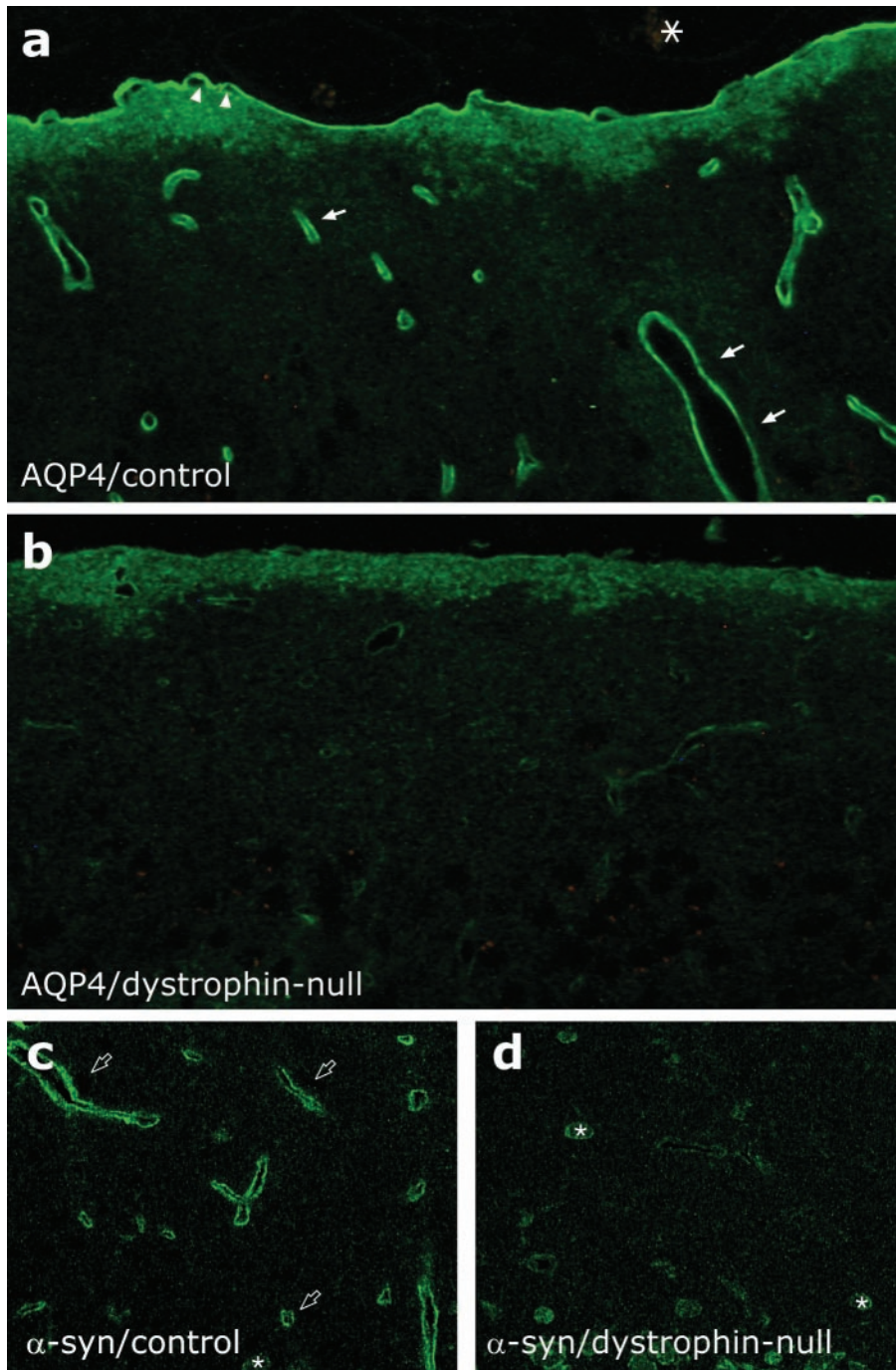††To whom reprint requests should be addressed. E-mail: sn@ana.au.dk.

MEDICAL SCIENCES

Fig. 1. Immunofluorescence localization of AQP4 and α-syn in brain. (*a*) In brain from G178 control mice, AQP4 labeling is concentrated in glial processes, forming the glia limitans (arrowheads) and surrounding intracerebral capillaries (arrows), but AQP4 labeling is not associated with neuronal elements or meninges (asterisk). (*b*) In brain from the dystrophin-null mice, AQP4 labeling is markedly decreased. (*c*) In brain from G178 control mice, α-syn is localized to the pericapillary glial end-feet (open arrows). (*d*) In brain from dystrophin-null mice, α-syn labeling of pericapillary astroglia is markedly reduced. Asterisks in *c* and *d* indicate labeling of α-syn in neuronal cells. (×250.)

cerebrum from the rhinal fissure to the level of the pineal gland, by a pulsed-gradient, spin-echo sequence with b values of 0 and 1,440 s/mm^2. The diffusion-sensitizing gradients were oriented parallel to the longitudinal axis of the brain. Additional imaging parameters were: slice thickness = 2 mm; field-of-view = 5.5 × 5.5 cm, 64 × 64 data matrix; number of acquisitions = 1; echo time = 50 ms; and repetition time = 1,200 ms.

Initially, three baseline DWI scans were made, and then the animal was removed from the magnet and subjected to i.p.

injection of distilled water (corresponding to 20% of body weight) together with 8-deamino-arginine vasopressin (0.3 μg/ kg). After the injection, the animal was repositioned carefully into the magnet and additional DWI scans were performed in 3.5-min intervals.

ADC maps were prepared on a pixel-by-pixel basis. Relative ADC maps then were calculated by normalizing the absolute ADC values, using the mean ADC value of the three baseline scans in each subject on a pixel-by-pixel basis. Mean relative
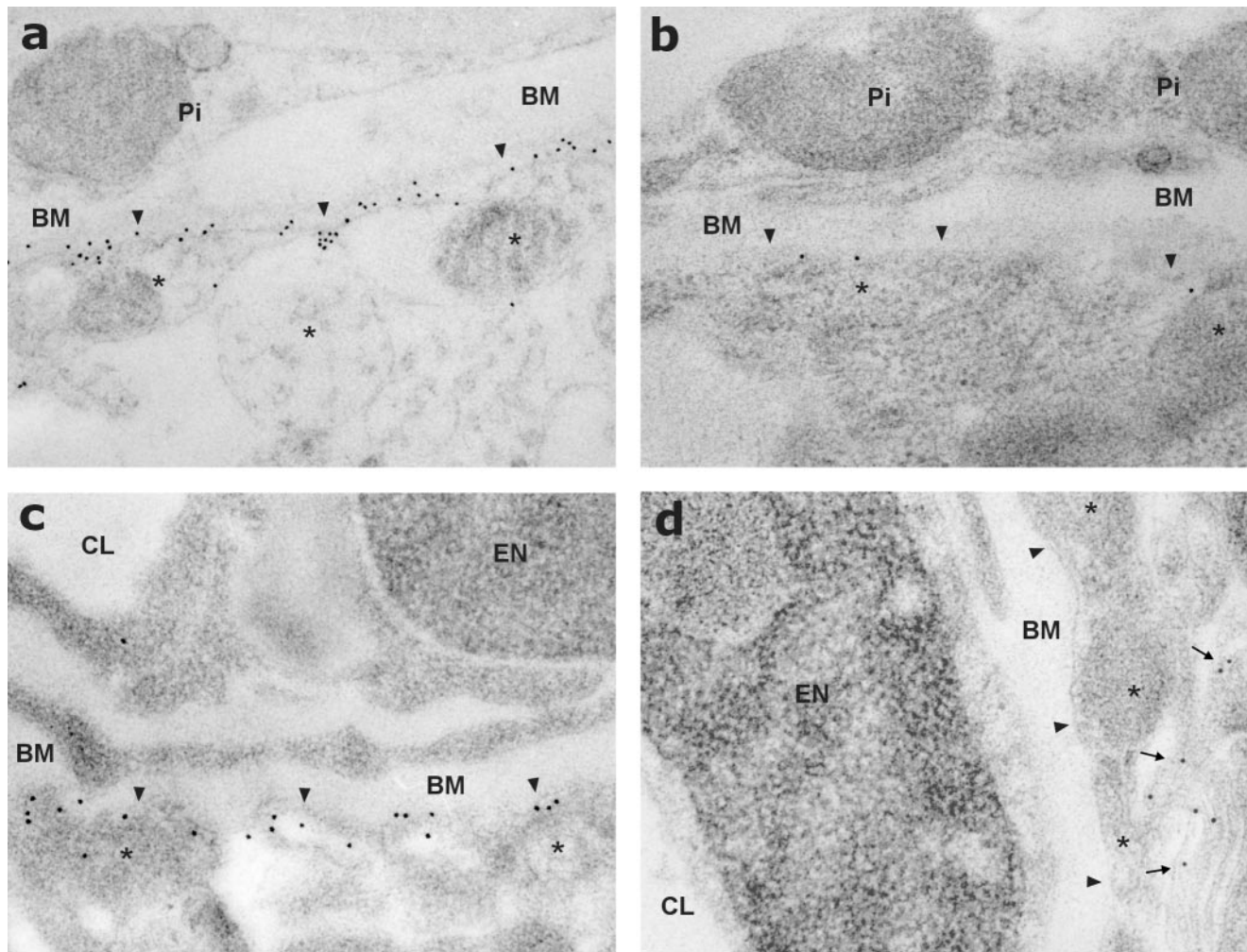
Vajda *et al.*

www.manaraa.com

Fig. 2. Postembedding immunogold electron-microscopic localization of AQP4 in brain. *a* and *b* correspond to glia limitans, and *c* and *d* correspond to pericapillary astroglial end-feet. (*a* and *c*) In brains of G178 control mice, AQP4 labeling is concentrated in glial processes (asterisks), forming the glia limitans (arrowheads in *a*) and surrounding intracerebral capillaries (arrowheads in *c*). (*b* and *d*) In brains of dystrophin-null mice, AQP4 labeling is markedly decreased in glia limitans (arrowheads in *b*) and pericapillary (arrowheads in *d*). The arrows in *d* indicate AQP4 in glial membrane domains apposed to adjacent glial or neuronal cells. Pi, cells of the pia mater; BM, basal membrane; CL, capillary lumen; EN, endothelial cell nucleus. (×16,000.)

ADC values of regions of interests, encompassing the whole brain, were obtained from the calculated relative ADC maps, and the mean value of all three slices has been used in the statistical analysis. Relative ADC values have been expressed as a percentage of the baseline level.

Antibodies. Polyclonal AQP4 antibody was raised in rabbit against a peptide corresponding to the C-terminal amino acids 280–296 (LL182) and affinity-purified as described in detail (5, 17). The monoclonal pan-syntrophin antibody (kind gift of S. Froehner, University of Washington, Seattle) has been characterized (for references, see ref. 7).

Preparation of Samples and Immunoblotting. Whole brains were homogenized, and the supernatant of a $4,000 \times g$ spin was used for immunoblotting (5, 3). Identical loading was assured by Coomassie blue staining. AQP4 protein levels in the dystrophin-null mice were calculated as a fraction of control levels, which were normalized to 100%.

Immunocytochemistry and Immunoelectron Microscopy. A parallel set of animals were anaesthetized deeply with pentobarbital sodium (7.5 mg/kg) and perfusion-fixed transcardially with 3%

or 4% paraformaldehyde in 0.1 M sodium cacodylate buffer, and the brains were removed and postfixed for 1 h and processed for immunofluorescence microscopy or postembedding immuno-electron microscopy, as described (3, 5).

Statistical Analysis. Values were presented as mean ± SEM. Comparisons between experimental groups were made by Student's unpaired *t* test. $P < 0.05$ was considered significant.

Results

Subcellular Localization of AQP4 in Brains of Dystrophin-Null Mice. Consistent with previous studies reporting the expression of the AQP4 protein in rat and mouse brain (3, 5–7), immunofluorescence and immunoelectron-microscopic analyses of brains from control animals revealed a highly polarized distribution of AQP4, with marked expression in astrocyte end-feet surrounding capillaries and forming the glia limitans at the surface of the brain (Figs. 1*a* and 2 *a* and *c*). No labeling was associated with meninges, vascular endothelial cells, or neuronal elements.

A dramatic reduction in the AQP4 labeling was observed at the cellular as well as the subcellular level in glial processes facing capillaries and glia limitans in sections from brains of dystrophin-null mice (Figs. 1*b* and 2 *c* and *d*). This was observed throughout
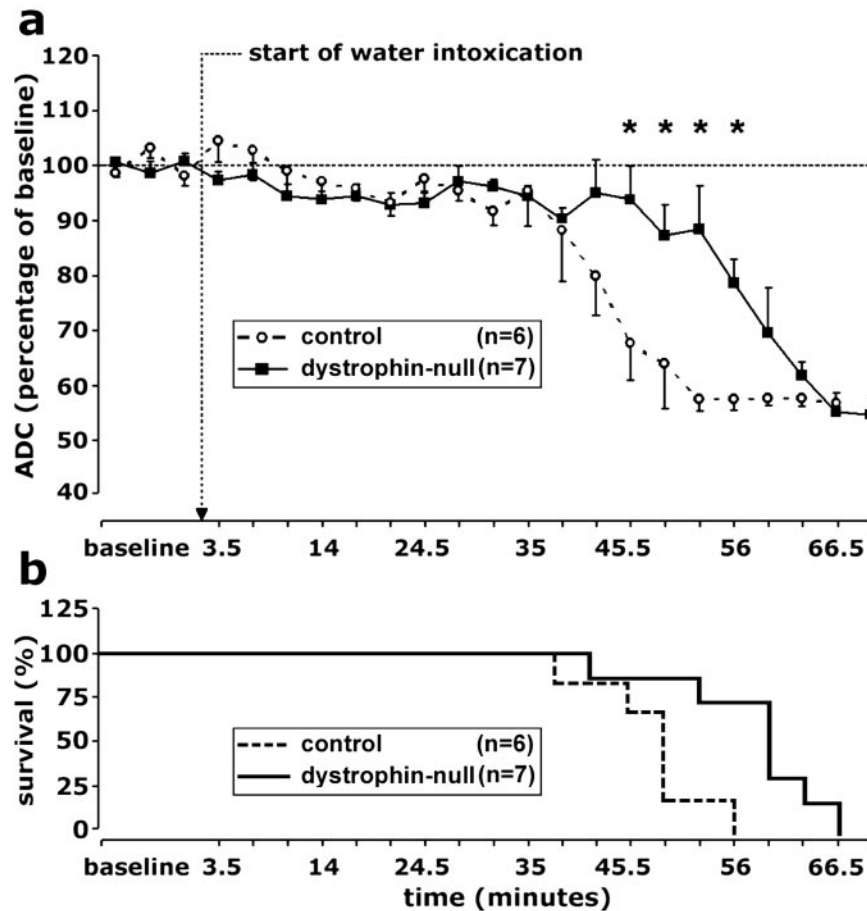
MEDICAL SCIENCES

Fig. 3. Time course of hyponatremia-induced brain edema. (*a*) Average ADC values in brain were normalized to the mean of baseline values. The arrow denotes i.p. injection of distilled water and 8-deamino-arginine vasopressin (water intoxication). Note that the gradual decline in ADC occurred in both experimental groups, indicating an increase in the size of the intracellular compartment. After 35 min, an abrupt, rapid decline in ADC occurred in the G178 control mice (○, broken line). After 52.5 min, a similar decline occurred in dystrophin-null mice (■, solid line). ∗, $P < 0.05$ (Student's *t* test). Data are presented as mean ± SE. (*b*) Survival profile for G178 control mice and dystrophin-null mice.

the whole brain including the cerebrum, cerebellum, and basal ganglia. Some labeling remained in glial membrane domains that do not face blood–brain and blood–CSF barriers.

α-Syn Localization in the Brain. Immunofluorescence microscopy of α-syn in control mice showed a localization pattern similar to that of AQP4, with marked expression in pericapillary astrocytic end-feet (Fig. 1*c*), as reported (7). In dystrophin-null animals, a marked decrease in the pericapillary abundance of α-syn was evident (Fig. 1*d*), indicating that targeting of α-syntrophins (including α1-syn) depends on the presence of dystrophin. These results are also consistent with the observed disruption of AQP4 targeting in α1-syn-null mice (7).

AQP4 Protein Levels in Brain. Immunoblotting with an antibody specific for the C terminus of AQP4 revealed bands of ≈32–34 kDa (data not shown) that corresponded to the M23 and M1 splice variants of the protein (5). Densitometric analysis revealed no differences in the abundance of brain AQP4 protein expression between controls (100.0% ± 5.8%) and dystrophin-null (100.8% ± 1.8%) mice. Thus, similar to the observations with α1-syn-null mice (7), absence of dystrophin causes mislocalization of AQP4 protein but does not alter its abundance.

Changes in Brain ADC After Water Intoxication. The mean absolute ADC values of the brain were determined (Fig. 4*a*). The ADC

values for control mice (646 ± 35 $\mu m^2/s$) were not significantly different from values determined for dystrophin-null mice (662 ± 15 $\mu m^2/s$). These values are consistent with previously reported absolute ADC values in mouse brain (19).

ADC determinations were measured at 3.5-min intervals after i.p. injection of water. Equivalent gradual declines were observed from the baseline ADC levels to 95% ± 6% (G178 control mice) and 94% ± 2% (dystrophin-null mice) during the first 35 min after the induction of water intoxication. Thus, the initial phases of intracellular water accumulation were similar in the two experimental groups (Figs. 3*a* and 4*b*). After 35 min, the control mice sustained a rapid decline in ADC that decreased from 88% ± 9% at 38.5 min to 58% ± 2% at 52.5 min after injection. By 56 min, all of the control animals were dead (Figs. 3*b* and 4*b*), as revealed by the absence of the minor motion artifacts that normally are present on the diffusion-weighted images because of respiratory movements.

The dystrophin-null animals showed a markedly different course (Figs. 3 and 4*b*). At 49 min after injection, five of six control mice already were dead, but only one dystrophin-null mouse had succumbed, and the mean ADC level remained high (87% ± 6%). After a consistent delay, the dystrophin null mice finally sustained a similar, rapid decline in ADC that decreased from 88% ± 8% at 52.5 min to 55% ± 3% at 66.5 min, when all of the dystrophin-null mice were dead. Thus, statistically significant differences in ADC measurements were identified when

the control mice and dystrophin-null values were compared at 45.5 ($P = 0.015$), 49 ($P = 0.037$), 52.5 ($P = 0.01$), and 56 min ($P = 0.002$) after injection.

To ensure the validity of the control determinations, non-transgenic age-matched, female NMRI mice were analyzed by immunohistochemistry and MRI experiments. No differences were observed between the Gl78 and NMRI mice in the subcellular localization of AQP4 protein. Likewise, virtually identical ADC values ($88\% \pm 9\%$ vs. $88\% \pm 3\%$, $57\% \pm 2\%$ vs. $61\% \pm 8\%$, and $57\% \pm 2\%$ vs. $61\% \pm 1\%$ at 38.5, 56, and 66.5 min, respectively) and survival rates were observed in the Gl78 ($n = 6$) and NMRI ($n = 5$) animals after water intoxication, without significant differences between the two strains.

Discussion

Here, we report the cellular and subcellular localization of the AQP4 water channel protein in astroglial membranes of transgenic dystrophin-null mice (*mdx-βgeo*). The gene for dystrophin is very important in clinical medicine, because it is the site of mutations in Duchenne and Becker muscular dystrophies. Moreover, dystrophin normally plays a key role in anchoring the extracellular matrix and membrane proteins to the cytoskeleton. Importantly, the *mdx-βgeo* mice used in this study bear a targeted disruption of the gene encoding dystrophin and fail to express any of its isoforms. We found that the abundance of AQP4 was reduced greatly in astroglial end-feet surrounding capillaries (blood–brain barrier) and forming the glia limitans (CSF–brain interface) throughout the whole cerebrum, cerebellum, and basal ganglia of the dystrophin-null mice. Because the overall abundance of AQP4 protein expression was not reduced, we conclude that AQP4 membrane trafficking is perturbed.

Multiple lines of research now indicate that the DAP complex is essential for proper localization of AQP4 protein in brain. Mislocalization of AQP4 was identified recently in brains of mice bearing targeted disruptions of the gene encoding α-syn (7), a component of the DAP complex. It was suggested that the PDZ (PSD95, Discs Large, Z01)-binding domain in the C terminus of AQP4 may associate with dystrophin through α-syn or possibly another DAP component. By immunocytochemical analyses with anti-pan-syntrophin antibody, we found decreased abundance of syntrophins in the brain (Fig. 1 *c* and *d*), confirming that the integrity of the DAP complex requires dystrophin. Nevertheless, it should be considered that expression of other membrane proteins also could be altered in dystrophin-null animals. A recent study by Knuesel *et al.* (20) reported alteration of synaptic clustering of GABA$_A$ receptors in mice, with a spontaneous mutation eliminating the full-length dystrophin isoform (mdx strain). Evidence for regulated degradation of AQP4 has been obtained in MDCK cells transfected with AQP4 constructs. Studies by Madrid *et al.* (21) revealed that phosphorylation of serine-276 by stress-induced kinase (casein kinase II) may target AQP4 to the late degradation compartments of the endocytic pathway. Additional studies are necessary to establish such a role for regulated trafficking of AQP4 in glial cells and whether this can be exploited *in vivo*. Importantly, Frigeri *et al.* (22) recently analyzed human muscle biopsies from different forms of muscular dystrophies and demonstrated that the expression and stability of α-syn in the sarcolemma is not always accompanied by decreases in AQP4. Thus, additional studies are needed to precisely define the relationship of AQP4 with components of the DAP complex in human brain.

Manley *et al.* (2) recently described a valuable protocol for inducing systemic hyponatremia, which we used in the present study. We used DWI to elucidate which effects the absence of AQP4 from the blood–brain barrier and the CSF–brain interface have on intracellular water accumulation during the development of brain edema. The water intoxication protocol induced an initial gradual decrease of the ADC, indicating a water shift
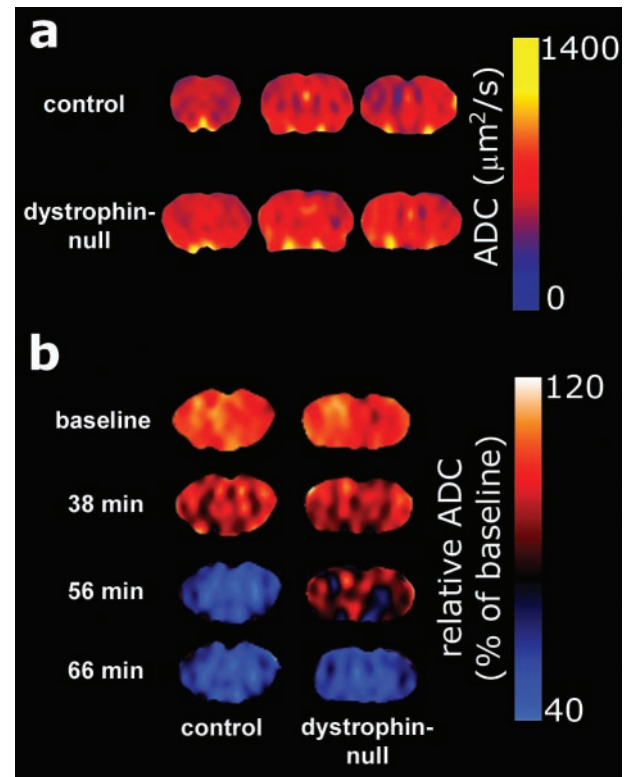

Fig. 4. Representative ADC and relative ADC maps of brains from G178 control mice and dystrophin-null mice. (*a*) ADC maps were calculated in three consecutive, 2-mm-thick slices, covering the majority of the brain. The profiles for both groups are similar. (*b*) Relative ADC maps were calculated by normalizing the absolute ADC values to the mean of the three baseline scans on a pixel-by-pixel basis. Note the delay in ADC decline in maps of dystrophin-null mice.

along the increasing osmotic gradient toward the intracellular compartment. The initial decrease in ADC was similar in control and dystrophin-null mice. The striking difference was that control mice abruptly decompensated 35 min after i.p. injection of distilled water, whereas a delay was noted before the dystrophin-null mice abruptly decompensated at 52.5 min. Although all animals in both groups eventually died, the consistent prolongation of survival by the dystrophin-null mice most likely is a result of the absence of AQP4 from its normal location.

The gradual decline in ADC noted for both groups of animals during the first 35 min after i.p. injection of water is puzzling. We recently identified a corresponding initial decrease in ADC in rats treated with a similar protocol (15). In the present study, both groups of mice exhibited similar, gradual decreases in ADC for up to 35 min, leading us to conclude that AQP4 protein in the pericapillary membrane domains does not cause the initial water influx into the intracellular space of the brain tissue in systemic hyponatremia. It is possible to assume that the initial gradual decrease in ADC represents a compensated state during which activation of volume-regulatory mechanisms maintain the intracellular space at a constant size despite the decrease in serum osmolarity. The abrupt decompensation may represent the point at which volume-regulatory mechanisms are exhausted. When this occurs, we hypothesize that the intracellular volume fraction expands rapidly, increasing the intracranial pressure and decreasing cerebral perfusion. The systemic hyponatremia protocol is uniformly lethal, with death presumably resulting from cerebral herniation. The median survival of control animals in our studies, 48 min, is very close to that reported by Manley *et*

MEDICAL SCIENCES

www.manaraa.com

al., 44 min (2). Thus, it is highly significant that survival is extended in both the dystrophin-null mice, lacking AQP4 in the astroglial end-feet, as well as mice totally lacking AQP4 protein. Differences in survival by the AQP4-null mice (2) and the dystrophin-null mice (the present study) may be a result of other factors. For example, AQP4 knockout mice may be partially resistant to systemic hyponatremia, because they lack the protein in the distal collecting duct (2), whereas AQP4 expression and localization are normal in the kidneys of dystrophin-null mice (not shown).

The results reported here suggest that interference with the localization of AQP4 at the blood–brain barrier and CSF–brain interface may confer resistance to the onset of brain edema. The possibility that this may provide a new therapeutic target is underscored by the known lability of PDZ (PSD95, Discs Large, Z01) domain associations. The observations reported here and other recently published studies (2, 7) all used mice bearing targeted gene disruptions, and it remains uncertain how this may be translated to human brain. Nevertheless, the devastating consequences that brain edema causes for human patients and the minimal repertoire of existing therapies strongly endorse the need for further investigation of AQP4 in brain.

1. Preston, G. M., Carroll, T. P., Guggino, W. B. & Agre, P. (1992) *Science* **256,** 385–387.
2. Manley, G. T., Fujimura, M., Ma, T., Noshita, N., Filiz, F., Bollen, A. W., Chan, P. & Verkman, A. S. (2000) *Nat. Med.* **6,** 159–163.
3. Vajda, Z., Promeneur, D., Dóczi, T., Sulyok, E., Frøkiaer, J., Ottersen, O. P. & Nielsen, S. (2000) *Biochem. Biophys. Res. Commun.* **270,** 495–503.
4. Venero, J. L., Vizuete, M. L., Machado, A. & Cano, J. (2001) *Prog. Neurobiol.* **63,** 321–336.
5. Nielsen, S., Nagelhus, E. A., Amiry-Moghaddam, M., Bourque, C., Agre, P. & Ottersen, O. P. (1997) *J. Neurosci.* **17,** 171–180.
6. Frigeri, A., Nicchia, G. P., Nico, B., Quondamatteo, F., Herken, R., Roncali, L. & Svelto, M. (2001) *FASEB J.* **15,** 90–98.
7. Neely, J. D., Amiry-Moghaddam, M., Ottersen, O. P., Froehner, S. C., Agre, P. & Adams, M. E. (2001) *Proc. Natl. Acad. Sci. USA* **98,** 14108–14113.
8. Neumann-Haefelin, T., Moseley, M. E. & Albers, G. W. (2000) *Ann. Neurol.* **47,** 559–570.
9. Barzó, P., Marmarou, A., Fatouros, P., Hayasaki, K. & Corwin, F. (1997) *J. Neurosurg.* **87,** 900–907.
10. Sevick, R. J., Kanda, F., Mintorovitch, J., Arieff, A. I., Kucharczyk, J., Tsuruda, J. S., Norman, D. & Moseley, M. E. (1992) *Radiology* **185,** 687–690.
11. Szafer, A., Zhong, J. & Gore, J. C. (1995) *Magn. Reson. Med.* **33,** 697–712.
12. Smouha, E. & Neeman, M. (2001) *Magn. Reson. Med.* **46,** 68–77.
13. Qiao, M., Malisza, K. L., Del Bigio, M. R. & Tuor, U. I. (2002) *Radiology* **223,** 65–75.
14. O'Shea, J. M., Williams, S. R., van Bruggen, N. & Gardner-Medwin, A. R. (2000) *Magn. Reson. Med.* **44,** 427–432.
15. Vajda, Z., Pedersen, M., Dóczi, T., Sulyok, E., Stødkilde-Jørgensen, H., Frøkiaer, J. & Nielsen, S. (2001) *Neurosurgery* **49,** 697–704.
16. Wertz, K. & Füchtbauer, E. M. (1998) *Dev. Dyn.* **212,** 229–241.
17. Terris, J., Ecelbarger, C. A., Marples, D., Knepper, M. A. & Nielsen, S. (1995) *Am. J. Physiol.* **269,** F775–F785.
18. Jung, J. S., Bhat, R. V., Preston, G. M., Guggino, W. B., Baraban, J. M. & Agre, P. (1994) *Proc. Natl. Acad. Sci. USA* **91,** 13052–13056.
19. van Dorsten, F. A., Hata, R., Maeda, K., Franke, C., Eis, M., Hossmann, K. A. & Hoehn, M. (1999) *NMR Biomed.* **12,** 525–534.
20. Knuesel, I., Mastrocola, M., Zuellig, R. A., Bornhauser, B., Schaub, M. C. & Fritschy, J. M. (1999) *Eur. J. Neurosci.* **11,** 4457–4462.
21. Madrid, R., Le Maout, S., Barrault, M. B., Janvier, K., Benichou, S. & Merot, J. (2001) *EMBO J.* **20,** 7008–7021.
22. Frigeri, A., Nicchia, G. P., Repetto, S., Bado, M., Minetti, C. & Svelto, M. (2002) *FASEB J.* **16,** 1120–1122.